frontiers

Supplementary Material

Uptake of Pu(IV) by hardened cement paste in the presence of gluconate at high and low ionic strengths

J. Stietz[1*], S. Amayri[1], V. Häußler[1], D. Prieur[2], T. Reich[1*]

[1] Department of Chemistry, Johannes Gutenberg-Universität Mainz, Mainz, Germany,

[2] Institute of Resource Ecology, Helmholtz-Zentrum Dresden-Rossendorf e.V., Dresden, Germany

*** Correspondence:** Janina Stietz: *jastietz@uni-mainz.de*

Tobias Reich: *treich@uni-mainz.de*

The supplementary material comprises 7 pages, including 4 tables, 4 figures, and 6 references.

Note: The order of the supplementary material is chronological, as cross references appear in the article.

SM-1. Chemical composition of ACW

The elemental concentrations in the artificial cement pore water (ACW) before and after contact with hardened cement paste (HCP) (S/L = 5 g L^{-1}) for 72 h, were identified by ICP-MS SemiQuant analysis (7900 Series ICP-MS, Agilent Technologies, United States). With the SemiQuant analysis mode of the ICP-MS (Octopol-Reaction-System), all elements of a solution can be determined by measuring a stock solution with specified concentrations of standards ([Li, Co, Y, Ce, Tl] = 1 ppb). In addition, an ^{193}Ir stock solution ([Ir] = 100 ppt) was used as internal standard. These stock solutions were prepared in 2% HNO_3. The uncertainty of this method is ~30%.

The measurements showed that elements are leached from HCP. Especially relevant for this work is the concentration of 3×10^{-3} M Ca^{2+}, which is in good agreement with a value of the literature ([Ca] = 1×10^{-3} M (Ochs et al., 2016)). The results are summarized in Supplementary Table S1.

Supplementary Table S1. Elemental concentrations in mol L^{-1} of ACW before and after contact with HCP.

	Na	Al	Si	S	K	Ca	Fe
ACW	1.2×10^{-1}	n.d.	3.3×10^{-4}	n.d.	1.4×10^{-1}	n.d.	2.8×10^{-7}
ACW*	1.4×10^{-1}	1.2×10^{-4}	4.3×10^{-4}	2.0×10^{-3}	2.2×10^{-1}	2.8×10^{-3}	2.1×10^{-6}

*) ACW after contact with HCP (5 g L^{-1}, 72 h).

SM-2. Chemical composition of ACW-VGL

The Supplementary Table S2 summarizes the chemical composition in terms of weight for the oxides of ACW-VGL (for preparation see Section 2.2) determined with XRF measurements (XRF spectrometer MagiXPRO, Philips, Netherlands). Rh was utilized as the anode with an excitation power of 3.6 kW. For the measurement, 30 mL ACW-VGL was dried for 72 h at 110 °C in the drying oven. The dried salt (4.5 g) was measured as a pellet. The uncertainty for the main elements is < 3%.

Supplementary Table S2. Chemical composition of ACW-VGL in weight-% for the oxides.

SiO_2	Al_2O_3	Fe_2O_3(t)	MnO	MgO	CaO	Na_2O	K_2O	TiO_2	P_2O_5	SO_3	Cl
0.047	0.016	0.028	0	0	0.751	49.050	0.112	0.011	0.007	0.020	43.3

Loss on ignition at 650 °C = 0.72 weight-%

SM-3. Speciation of gluconate in ACW and ACW-VGL

Supplementary Figure S1 shows the calculated speciation of 1×10^{-2} M gluconate (GLU) in ACW (left) and ACW-VGL (right). At pH ≥ 12.5 the concentration of the species Ca(OH)(HGLU) is somewhat larger in ACW-VGL than in ACW due to different Ca^{2+} concentrations in both electrolytes.

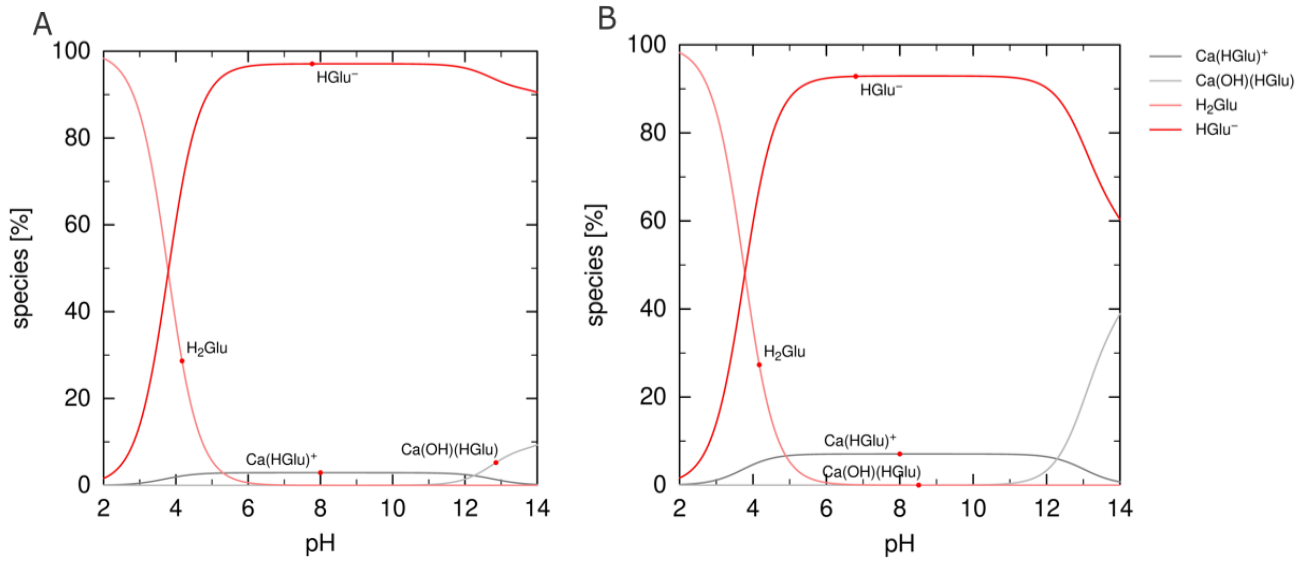

Supplementary Figure S1. Speciation calculation for 1×10^{-2} M GLU in ACW (A) and ACW-VGL (B). (Graphic generated by PhreePlot (version 1.0 (Parkhurst and Appelo, 2016)) using PHREEQC and the ThermoChimie database 9b0, 2015 (Giffaut et al., 2014)).

SM-4. Complex formation constants

Supplementary Table S3. Thermodynamic data used for the equilibria calculations of Pu(IV) in presence and absence of GLU from the ThermoChimie database 9b0, 2015 (Guillaumont et al., 2003; Gaona et al., 2008; Giffaut et al., 2014).

Chemical equilibrium	log K^0
$Pu^{4+} + 4\,H_2O \rightleftharpoons Pu(OH)_4\,(aq) + 4H^+$	-8.50 ± 0.50
$Pu^{4+} + HGlu^- + 3\,H_2O \rightleftharpoons Pu(OH)_3(HGlu) + 3H^+$	4.75 ± 1.50
$Pu^{4+} + HGlu^- + 4\,H_2O \rightleftharpoons Pu(OH)_4(HGlu)^- + 4H^+$	-2.70 ± 1.50

SM-5. Pu(IV) speciation in ACW/ACW-VGL in presence of GLU

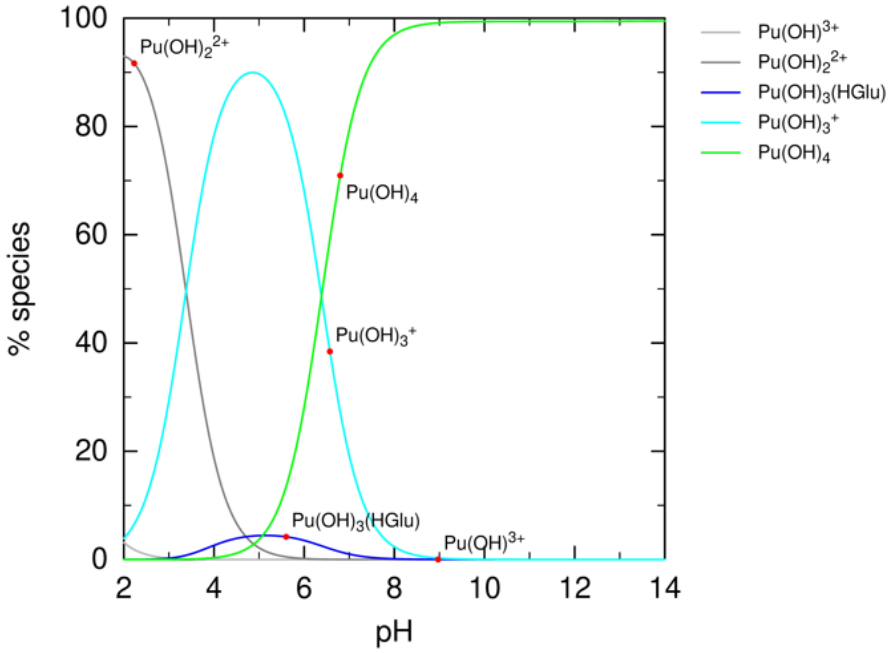

Supplementary Figure S2. Speciation calculation for 1×10^{-8} M Pu(IV) and 1×10^{-8} M GLU in ACW. (Graphic generated by PhreePlot (version 1.0 (Parkhurst and Appelo, 2016)) using PHREEQC and the ThermoChimie database 9b0, 2015 (Giffaut et al., 2014)).

SM-6. Modelling of sorption isotherms of GLU on HCP

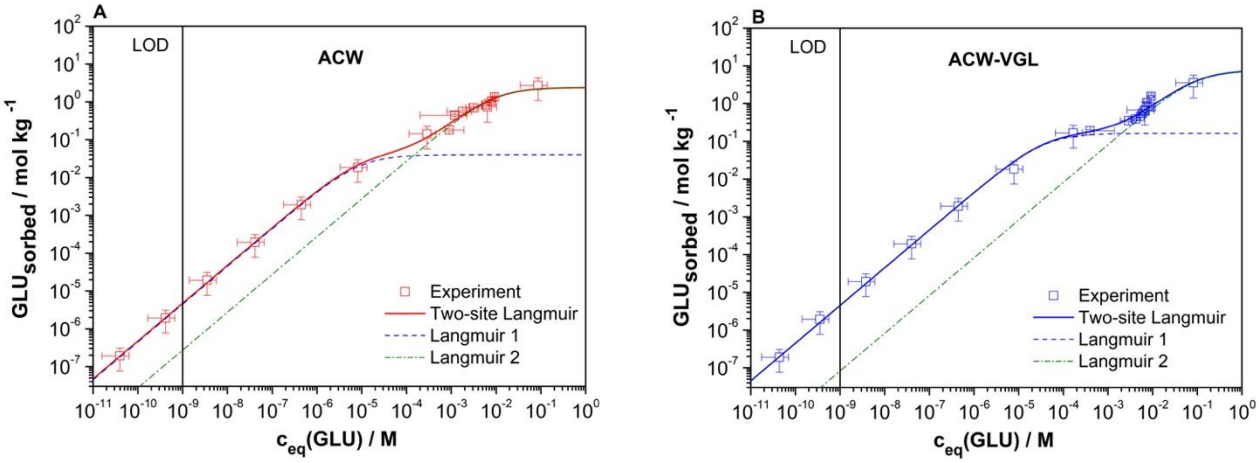

Supplementary Figure S3. Modelling of GLU sorption isotherms on HCP in ACW (A) and ACW-VGL (B), respectively, using a two-site Langmuir-isotherm. The dashed lines represent the components of the two-site Langmuir-isotherm. Their sums are shown as solid lines.

SM-7. Analysis of the deglitches Pu L_{III}-edge EXAFS spectra

Since all raw data showed a strong intensity variation, a so-called monochromator glitch, in the energy range from 18284.6 eV to 18299.9 eV, an attempt was made to deglitch the raw Pu L_{III}-edge XAFS data using the software package EXAFSPAK (George and Pickering, 2000). The five data points in this energy range were interpolated by a cubic through the middle of two points on either side of the glitch. The deglitched k^3-weighted EXAFS spectra are shown in Supplementary Figure S4. Note the spectral change in the *k*-range from 7.7 to 7.9 $Å^{-1}$ compared to the raw data shown in Figure 4 of the article. The structural parameters of the best model to the deglitched EXAFS spectra are given in Supplementary Table S4 and can be compared to the corresponding model for the raw data (see Table 6 of the article). The data were fitted in the *k*-range from 2.1 to 10.9 $Å^{-1}$. The shift in E_0 energy, ΔE_0, was the only variable that was varied as one global parameter for all coordination shells. All other variables were allowed to vary freely.

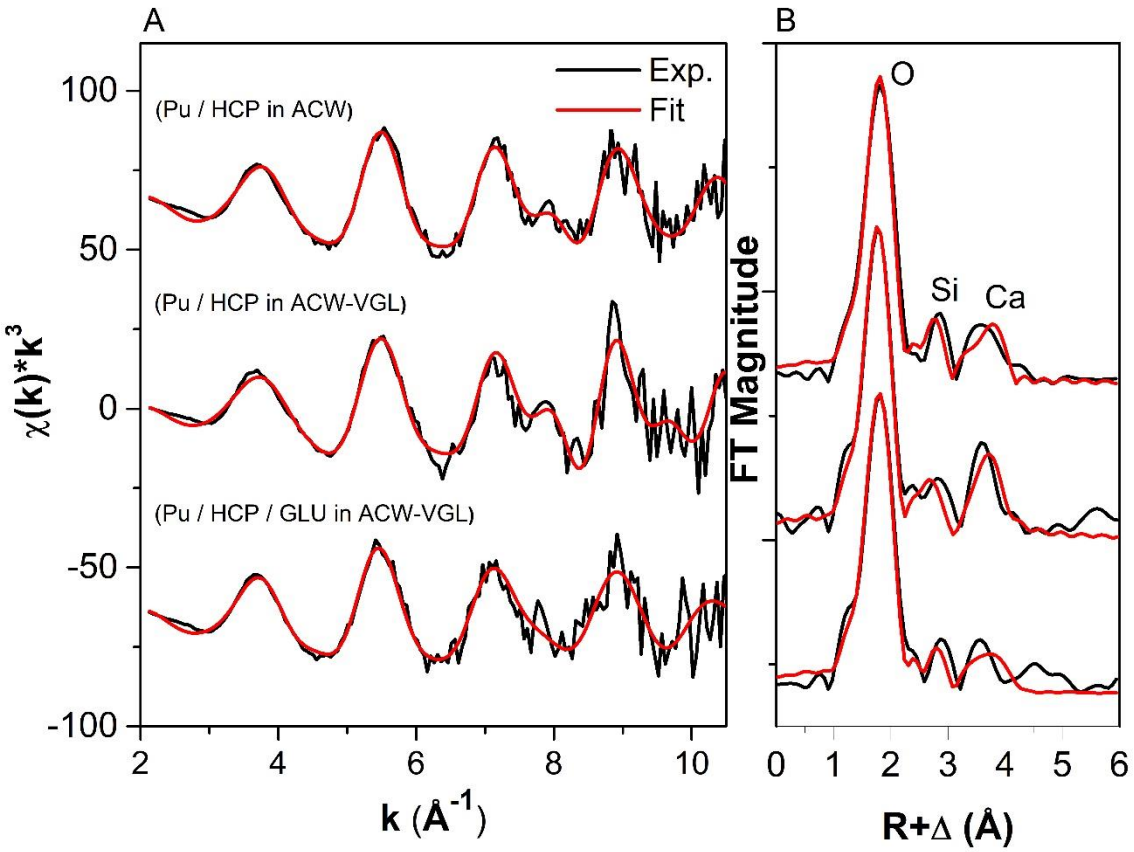

Supplementary Figure S4. Deglitched Pu L_{III}-edge k^3-weighted EXAFS spectra (A) of Pu loaded on HCP and the corresponding Fourier transform magnitude (B). Black line: experimental; red line: best model.

Supplementary Table S4. EXAFS structural parameters obtained from deglitched Pu L_{III}-edge k^3-weighted EXAFS spectra. N – coordination number, R – distance in Å, and σ^2 – Debye-Waller factor in $Å^2$, $S_0^2 = 0.9$.

Sample	Shell	N	R	σ^2
Pu / HCP / ACW	Pu-O	6.2 ± 0.3	2.281 ± 0.004	0.009 ± 0.001
(norm. error = 0.2, ΔE_0 = 2.2 ± 0.4 eV)	Pu-Si	1.0 ± 0.3	3.14 ± 0.01	0.005 ± 0.002
	Pu-Ca	5.2 ± 1.4	4.18 ± 0.01	0.012 ± 0.003
Pu / HCP / ACW-VGL	Pu-O	6.0 ± 0.3	2.261 ± 0.004	0.009 ± 0.001
(norm. error = 0.4, ΔE_0 = 0.1 ± 0.5 eV)	Pu-Si	1.6 ± 0.5	3.14 ± 0.01	0.007 ± 0.003
	Pu-Ca	2.4 ± 0.7	4.16 ± 0.01	0.002 ± 0.002
Pu / HCP /GLU / ACW-VGL	Pu-O	6.4 ± 0.3	2.285 ± 0.004	0.010 ± 0.001
(norm. error = 0.3, ΔE_0 = 1.4 ± 0.4 eV)	Pu-Si	0.7 ± 0.4	3.16 ± 0.01	0.005 ± 0.004
	Pu-Ca	11.7 ± 4.7	4.18 ± 0.02	0.027 ± 0.006

References

Gaona, X., Montoya, V., Colàs, E., Grivé, M., and Duro, L. (2008). Review of the complexation of tetravalent actinides by ISA and gluconate under alkaline to hyperalkaline conditions. *J. Contam. Hydrol.* 102**,** 217-227.

George, G.N., and Pickering, I.J. (2000). EXAFSPAK - A suite of computer programs for analysis of X-ray absortion spectra. *Stanford Synchrotron Radiation Lightsource*.

Giffaut, E., Grivé, M., Blanc, P., Vieillard, P., Colàs, E., Gailhanou, H., Gaboreau, S., Marty, N., Madé, B., and Duro, L. (2014). Andra thermodynamic database for performance assessment: ThermoChimie. *Appl. Geochem.* 49**,** 225-236.

Guillaumont, R., Fanghänel, T., Fuger, J., Grenthe, I., Neck, V., Palmer, D.A., and Rand, M.H. (2003). *Update on the Chemical Thermodynamics of Uranium, Neptunium, Plutonium, Americium and Technetium.* Paris: OECD Publishing.

Ochs, M., Mallants, D., and Wang, L. (2016). *Radionuclide and Metal Sorption on Cement and Concrete.* Springer International Publishing Switzerland.

Parkhurst, D.L., and Appelo, C.a.J. (2016). *PHREEQC (Version 3.3.5) - A computer program for speciation, batch-reaction, one-dimensional transport, and inverse geochemical calculations* [Online]. Available: http://wwwbrr.cr.usgs.gov/projects/GWC_coupled/phreeqc/index.html [Accessed 2023].